Research Square

Preprints are preliminary reports that have not undergone peer review.
They should not be considered conclusive, used to inform clinical practice,
or referenced by the media as validated information.

Role of Cu Layer on the Enhancement of Spin-to-Charge Conversion in Py/Cu/Bi_2Se_3

Shu Hsuan Su
National Cheng Kung University
Cheong-Wei Chong
National Cheng Kung University
Yu-Xiang Huang
National Cheng Kung University
Yi-Chun Chen
National Cheng Kung University
Vyacheslav Viktorovich Marchenkov
M.N. Miheev Institute of Metal Physics
Jung-Chun Andrew Huang (jcahuang@mail.ncku.edu.tw)
National Cheng Kung University

Research Article

Keywords: spin-to-charge conversion, topological insulator, spin pumping

Posted Date: May 6th, 2021

DOI: https://doi.org/10.21203/rs.3.rs-494900/v1

License: This work is licensed under a Creative Commons Attribution 4.0 International License.
Read Full License

Abstract

The enhancement of spin-to-charge conversion in Py/Cu/Bi_2Se_3 is achieved when increasing the Cu layer thickness up to 7nm. The conversion rate is studied using spin pumping technique. The inverse IEE length λ_{IEE} is found to increase up to ~2.7nm when 7nm Cu layer is introduced. Interestingly, maximized λ_{IEE} is obtained when the effective spin mixing conductance (and thus J_s) is decreased due to the Cu insertion. Monotonic increase of λ_{IEE} with decreasing J_s suggests that IEE relaxation time τ is enhanced due to additional tunnelling barrier (Cu) that limits the interface transmission rate. The results have shown the importance of interface engineering in Py/TI magnetic heterostructure, which is the key factor for optimizing spin-to-charge conversion efficiency.

Introduction

Manipulation of spin current by electrical charges or voltages is one of the key subjects for new generation of spintronic devices. Three dimensional (3D) topological insulators (TI) are great candidate for spintronic applications, since their spin-momentum locked properties enable spin accumulation on the surface by passing electrical charge current through the TI channel.[1,2] In addition, the degree of spin polarization can be further manipulated by controlling the Fermi level.[3,4] Owing to the spin momentum locking, 3D spin current density J_s injected onto TI surface will produce 2D charge density J_c on TI surface states (SS), so-called inverse Edelstein effect (IEE). The inverse IEE length λ_{IEE} is determined as J_c/J_s and can be experimentally probed using spin pumping technique.[5,6,7,8]

Numerous studies have been reported for determining the spin-to-charge conversion efficiency in 3D TI.[5,9,10,11] Particularly, giant spin hall angle (SHA) as large as ~0.43 was reported in Bi_2Se_3 that attributed to the enhanced spin current by the surface states and then converted into dc-voltage due to the bulk inverse spin hall effect.[9] However, large variations of SHA was found, which is an order of magnitude difference and the authors ascribed such variation to the non-uniformity of interface quality.[9] On the other hand, Wang et al. observed the dominant role of surface states in spin-to-charge conversion, despite the unavoidable conducting bulk in Bi_2Se_3.[5] The effective spin mixing conductance was not increased monotonically although the thickness of Bi_2Se_3 varied from 2 QL to 60 QL, suggesting surface states dominated mechanism.[5] Obviously, the spin pumping characteristic are important parameters for investigating the spin-to-charge conversion mechanism in 3D TI, where controlling the interfacial properties are necessary steps.

Cu is widely used to control the spin transmissivity in the multilayer devices.[12,13,14] Du et al. demonstrated that the insertion of Cu layer between $Y_3Fe_5O_{12}$ (YIG) and W substantially improved the spin current injection into W, while similar insertion between YIG and Pt degraded the spin current.[13] The authors reported the quantitative analysis and found that the spin transport efficiency in heterostructures depends on spin conductance of each constituents and their interfaces.[13] Similar results were also

reported by Deorani et al. where the effect of Cu interlayer on spin mixing conductance indeed material dependent (Pt versus Ta).[14] Recently Cu layer was deposited on TI film in order to eliminate the proximity induced ferromagnetism in the spin-orbit torque (SOT) devices.[1,15] Despite the fact that Cu is the most common used spacer layer in the spintronic devices, there is still lacking of quantitative studies about the role of Cu insertion on spin-to-charge conversion in TI that measured based on spin pumping mechanism. In this work, we fabricated trilayer structure of Py/Cu/Bi_2Se_3 (Fig. 1) and studied the spin pumping characteristic by varying the Cu layer thickness. Cu layer is used to protect the TI surface from exchange interaction with Py. Our results imply that Cu also acts as the barrier to spin transmission into TI film. More importantly, spin-to-charge conversion efficiency was enhanced due to the introduction of Cu barrier. The related mechanism is discussed in this work.

Results And Discussion

Figure 2a shows the dc voltage as a function magnetic field H that measured at excitation frequency of 3GHz for sample Py/Cu(7nm)/Bi_2Se_3. The results for other frequencies can be found in Figure S2. The voltage signals consisting of symmetric (V_s) and antisymmetric (V_{as}) parts, which can be isolated by fitting the measured voltage (data curve) with the form

$$V = \frac{V_s(\Delta H)^2}{((\Delta H)^2+(H-H_r)^2)} + \frac{V_{as}(\Delta H(H-H_r))}{((\Delta H)^2+(H-H_r)^2)}$$

Here Hr is the FMR resonant field and ΔH is the line width of the signal. V_s is attributed to the injected spin current whereas V_{as} originated from anisotropic magnetoresistance (AMR) or anomalous Hall effect (AHE). Similar fitting is also done for other samples and V_s is extracted as shown in Figure 2b. It was found that V_s is larger in the presence of Cu layer. FMR experiments were also conducted as shown in Figures 2c and 2d. Figure 2d presents the frequency dependence of FMR line width for samples with different Cu thickness. The linear fitted slope is larger for bilayer and trilayer samples (Cu0, Cu3 and Cu7 denote t_{Cu}=0, 3, 7nm respectively) in comparison to single Py, indicating spin current injected into Bi_2Se_3, resulting in the broadening of the FMR line width and thus larger damping constant a. Interestingly, the $a_{Py/Cu/TI}$ was found decreases from 0.01262 to 0.01185 when increasing the thickness of Cu layer up to 7nm.

The resistance of the multilayer samples R_d were measured using four probe method. J_c is determined as $J_c = I_c/w = V_s/wR_d$, where w and I_c are the width of the sample and charge current as shown in Figure 3a. We used the standard analysis of spin pumping on TI[5,6,7] to evaluate the spin-to-charge conversion J_c/J_s. Spin mixing conductance G_{eff}^{-} which is used to illustrate the efficiency of generating spin current is extracted using Equation (1):

$$G_{eff}^{\uparrow\downarrow} = \frac{4\pi\, t_{Py} M_s}{g\, u_B} \Delta\alpha \qquad (1)$$

where M_s is saturation magnetization of Py, t_{Py} is thickness of Py and g is Landé factor and u_B is the Bohr magneton. M_s is calculated using Kittel formula from *f* vs. H_r (Figure 2c). Da = $a_{Py/Cu/TI}$ - a_{Py} and is determined by analysing DH_{pp} vs. *f* as shown in Figure 2d. For the spin current densities that injected across the interface due to spin pumping, Equation (2) is utilized as shown below:

$$J_s^{3D} = \frac{G_{eff}^2 \gamma^2 \hbar\, h_{rf}^2}{8\,\pi\,\alpha^2} \left(\frac{4\pi M_s \gamma + \sqrt{(4\pi M_s \gamma)^2 + 4\omega^2}}{(4\pi M_s \gamma)^2 + 4\omega^2} \right) \frac{2e}{\hbar} \qquad (2)$$

in which *g* is gyromagnetic ratio, w(=2pf) and h_{rf} are frequency and amplitude of microwave magnetic field respectively. The calculated J_s is presented in Figure 3b. By dividing J_c with J_s, spin-to-charge conversion efficiency J_c/J_s can be determined as shown in Figure 3c.

Figure 3a plots the J_c against t_{Cu}. There is an optimized J_c at thickness of 3 and 7nm. In contrast, J_s is reduced when 3 and 7nm Cu were incorporated. The trend of J_s vs t_{Cu} is consistent with the changes of $a_{Py/Cu/TI}$, where effective damping constant is found decreases when 3 and 7nm Cu were introduced. Interestingly, a maximized J_c/J_s is observed at t_{Cu}=7nm, where J_c/J_s reaches ~2.7nm. This result suggests that the optimization of J_c/J_s could be related to the decrease of J_s due to the Cu insertion. To investigate the possible reason for the J_c/J_s enhancement, we plot J_c/J_s as a function of effective spin mixing conductance $G_{eff}^{\uparrow\downarrow}$ as shown in Figure 4a. Various $G_{eff}^{\uparrow\downarrow}$ values were obtained by changing the Cu layer thickness. Large J_c/J_s is obtained at low value of $G_{eff}^{\uparrow\downarrow}$ (and thus minimum J_s as shown in Figure 3b). We further examined the J_c vs. $G_{eff}^{\uparrow\downarrow}$ as shown in Figure 4b. There is no enhancement of J_c with increasing $G_{eff}^{\uparrow\downarrow}$, revealing the spin-to-charge mechanism may not be dominated by the bulk spin hall effect (SHE).[14] Hence, we here suggest that the spin-to-charge conversion in our Py/Cu/TI system arises from inverse Edelstein effect, where the origin is the spin-momentum locked surface states of TI layer, same interpretation as other literatures.[5,11]

Low $G_{eff}^{\uparrow\downarrow}$ indicates strong spin backflow and spin memory loss (spin absorption) at the high SOC interface.[16,17] Both factors are relevant in this Py/Cu/TI trilayer system. If we examine $G_{eff}^{\uparrow\downarrow}$ (Py/Cu/TI) at various t_{Cu}, as presented in Figure 4c, except for Py/Cu(3nm)/TI and Py/Cu(7nm)/TI, samples Py/TI, Py/Cu(9nm)/TI and Py/Cu(11nm)/TI exhibit $G_{eff}^{\uparrow\downarrow} \sim 1.25 \times 10^{19}$ m^{-2}, which is the typical value for metal-metal interfaces.[18,19] As reported by Du et al., the effective spin mixing conductance of trilayer system (FM/Cu/NM, FM denotes ferromagnetic while NM denotes nonmagnetic material) is determined by the serial contribution of the two interfaces (FM/Cu and Cu/NM) and the spin resistance of Cu.[13] Here we

refer FM to Py while NM to TI film. One of the reason for the lower G_{eff}^{-} compared with $G_{Py/TI}^{-}$ may be resulted from smaller spin conductance $g_{Cu/TI}$ of Cu/TI than that of $G_{Py/TI}^{-}$, similar to the case in Cu/Pt.[13,14] However, since G_{eff}^{-} » $G_{Py/TI}^{-}$ at t_{Cu} ³9nm, here we assume Cu/TI and Py/Cu present similar quality with $G_{Py/Cu}^{-}$ » $g_{Cu/TI}$. Thus, by assuming degree of spin absorption at Cu/TI interfaces are similar in all cases, we suggest that the reason for lower G_{eff}^{-} of 3nm and 7nm Cu-based trilayer samples could be due to the strong spin accumulation at this ultrathin regime.[13] Stronger spin backflow occurs, as compared to t_{Cu}³9nm, which eventually leads to reduction of G_{eff}^{-}.

The decrease of G_{eff}^{-} seems have strong correlation to the spin-to-charge conversion efficiency. The next question is how such condition could increase the J_c/J_s? Here we defined J_c/J_s as $l_{IEE} = n_f t$ where n_f is Fermi velocity of TI surface states and t is IEE relaxation time. As shown in the Figure 4d, t is modified due to the tunnelling current into TI, which is determined by momentum relaxation time t_p and interface tunnelling time t_t as shown in Equation (3):[20]

$$\lambda_{IEE} = v_f \tau = v_f \frac{\tau_p}{\left(1+\frac{2\tau_p}{\tau_t}\right)} \quad (3)$$

where $l_{mf} = n_f t_p$ = mean free path TI. According to this model, we proposed that the monotonic increase of l_{IEE} with decreasing G_{eff}^{-} attributed to the modification of IEE relaxation time t due to additional tunnelling barrier (Cu) that limits the interface transmission rate ($1/t_t$).[20,21] l_{IEE} is always lower than l_{mf} due to the correction factor of ($1+2t_p/t_t$). It becomes clear that one can increase l_{IEE} by reducing $1/t_t$, which can be done by introducing tunnelling barrier in between Py and TI layer. Using l_{IEE} (t_{Cu}=7nm) =2.7nm and based on our previous ARPES result, n_f=5.7´10^5 m/s,[22] we find t~4.7*f*s, which is same order of magnitude as Bi/Ag[23] and a-Sn/Ag[6] interfaces. Our extracted l_{IEE}(=2.7nm) is higher than 0.1-0.4nm in Bi/Ag Rashba interface,[23] 2.1nm and 2nm in TI SS of a-Sn/Ag[6] and HgTe/HgCdTe[7] respectively. We attribute the enhancement to the insertion of Cu tunnelling barrier. Although more theoretical calculation might be needed, our works indicate the importance of interface engineering to enhance the spin-to-charge conversion. This method could also be applied to other high SOC interfaces for obtaining high spin-to-charge conversion based on the inverse Edelstein effect, which is essential for spin current detector and other novel application such as broadband terahertz emitter.[24,25]

Conclusion

In conclusion, we investigated the spin-to-charge conversion in Py/Cu/Bi_2Se_3 using spin pumping technique. Enhancement of J_c/J_s with increasing t_{Cu} is observed at room temperature, where J_c/J_s ~2.7nm is achieved when 7nm of Cu layer is inserted. We proposed that the enhancement is attributed to the additional Cu interlayer as tunnelling barrier that modified the relaxation time at the interface. This work has provided a viable route for enhancing spin-to-charge conversion efficiency of TI, which is crucial for spin functional device applications.

Materials And Methods

Bi_2Se_3 films with 10nm thickness were synthesized using molecular beam epitaxy (MBE) method. The as-grown Bi_2Se_3 were *in situ* capped with 2nm Se film that used as protecting layer. The sample was then transferred to pulse laser deposition (PLD) chamber for depositing Cu and subsequently NiFe (Py) layer at room temperature. Before the depositions, Se layer was decapped in PLD chamber at 183°C for 1 hour. A series of trilayer samples were prepared by varying Cu thickness, ranging from 3 to 11nm. Bilayer of Py/Bi_2Se_3 was also prepared for comparison study. Py thickness was fixed at 17 nm. 1 nm of Al film was deposited on Py as capping layer. To evaluate spin-to-charge conversion, spin pumping technique was utilized (Fig. 1). Spin current was generated in Py via its ferromagnetic resonance (FMR) condition and injected into Bi_2Se_3, either with or without passing through the Cu layer (-z direction) (Fig. 1b). DC voltage was measured in x-direction and the produced charge current could be evaluated. All the measurements were done at room temperature.

Declarations

Acknowledgments

This work was supported by the Ministry of Science and Technology, R.O.C. (Grants No MOST 107-2119-M-006-016-MY3).

Author contributions

S. H. S. and C.-W. C. designed the experiment flow, analyzed data, and wrote the main manuscript. Y.-X. H. grew the samples and performed the measurement. Y.-C. C. and V. V. M. provided useful discussion. J.-C.-A. H. financed the funding for this research.

Competing financial interests: The authors declare no competing financial interests.

References

1. R. Mellnik, J. S. Lee, A. Richardella, J. L. Grab, P. J. Mintun, M. H. Fischer, A. Vaezi, A. Manchon, E.-A. Kim, N. Samarth and D. C. Ralph, Spin-transfer torque generated by a topological insulator. *Nature* 511, 449 (2014).

2. Wang, D. Zhu, Yang Wu, Y. Yang, J. Yu, R. Ramaswamy, R. Mishra, S. Shi, M. Elyasi, K.-L. Teo, Y. Wu and H. Yang, Room temperature magnetization switching in topological insulator-ferromagnet heterostructures by spin-orbit torques. *Nat. Commun.* 8, 1364 (2017).
3. Neupane, A. Richardella, J. Sánchez-Barriga, S.Y. Xu, N. Alidoust, I. Belopolski, C. Liu, G. Bian, D. Zhang, D. Marchenko, A. Varykhalov, O. Rader, M. Leandersson, T. Balasubramanian, T.-R. Chang, H.-T. Jeng, S. Basak, H. Lin, A. Bansil, N. Samarth and M. Z. Hasan, Observation of quantum-tunnelling-modulated spin texture in ultrathin topological insulator Bi_2Se_3films. *Nat. Commun*. 5, 3841 (2014).
4. S. Lee, A. Richardella, D. R. Hickey, K. A. Mkhoyan, and N. Samarth, Mapping the chemical potential dependence of current-induced spin polarization in a topological insulator. *Phys. Rev. B* **92**, 155312 (2015).
5. Wang, J. Kally, J. S. Lee, T. Liu, H. Chang, D. R. Hickey, K. A. Mkhoyan, M. Wu, A. Richardella, and N. Samarth, Surface-State-Dominated Spin-Charge Current Conversion in Topological-Insulator–Ferromagnetic-Insulator Heterostructures. *Phys. Rev. Lett.* **117**, 076601 (2016).
6. -C. Rojas-Sánchez, S. Oyarzún, Y. Fu, A. Marty, C. Vergnaud, S. Gambarelli, L. Vila, M. Jamet, Y. Ohtsubo, A. Taleb-Ibrahimi, P. Le Fèvre, F. Bertran, N. Reyren, J.-M. George, and A. Fert,Spin to Charge Conversion at Room Temperature by Spin Pumping into a New Type of Topological Insulator: α-Sn Films. *Phys. Rev. Lett.* **116**, 096602 (2016).
7. Noel, C. Thomas, Y. Fu, L. Vila, B. Haas, P-H. Jouneau, S. Gambarelli, T. Meunier, P. Ballet, and J. P. Attané,Highly Efficient Spin-to-Charge Current Conversion in Strained HgTe Surface States Protected by a HgCdTe Layer. *Phys. Rev. Lett.* **120**, 167201 (2018).
8. Ohshima, Y. Ando, K. Matsuzaki, T. Susaki, M. Weiler, S. Klingler, H. Huebl, E. Shikoh, T. Shinjo, S. T. B. Goennenwein, and M. Shiraishi, Strong evidence for *d*-electron spin transport at room temperature at a $LaAlO_3/SrTiO_3$interface. *Nat. Mater.* 16, 609 (2017).
9. Jamali, J. S. Lee, J. S. Jeong, F. Mahfouz, Y. Lv, Z. Zhao, B. K. Nikolić, K. A. Mkhoyan, N. Samarth, and J.-P. Wang, Giant Spin Pumping and Inverse Spin Hall Effect in the Presence of Surface and Bulk Spin–Orbit Coupling of Topological Insulator Bi_2Se_3. *Nano Lett.* 15, 7126 (2015).
10. Deorani, J. Son, K. Banerjee, N. Koirala, M. Brahlek, S. Oh, and H. Yang, Observation of inverse spin Hall effect in bismuth selenide. *Phys. Rev. B* **90**, 094403 (2014).
11. B. S. Mendes, O. Alves Santos, J. Holanda, R. P. Loreto, C. I. L. de Araujo, Cui-Zu Chang, J. S. Moodera, A. Azevedo, and S. M. Rezende, Dirac-surface-state-dominated spin to charge current conversion in the topological insulator (Bi0.22Sb0.78)2Te3films at room temperature. *Phys. Rev. B* **96**, 180415(R) (2017).
12. Tserkovnyak, A. Brataas, and G. E. W. Bauer, Spin pumping and magnetization dynamics in metallic multilayers. *Phys. Rev. B* **66**, 224403 (2002).
13. Du, H. Wang, F. Yang, and P. C. Hammel, Enhancement of Pure Spin Currents in Spin Pumping Y3Fe5O12/Cu/MetalTrilayers through Spin Conductance Matching. *Phys. Rev. Appl.* **1**, 044004 (2014).

14. Deorani, and H. Yanga, Role of spin mixing conductance in spin pumping: Enhancement of spin pumping efficiency in Ta/Cu/Py structures. *Appl. Phys. Lett.* **103**, 232408 (2013).
15. Kondou, R. Yoshimi, A. Tsukazaki, Y. Fukuma, J. Matsuno, K. S. Takahashi, M. Kawasaki, Y. Tokura, and Y. Otani, Fermi-level-dependent charge-to-spin current conversion by Dirac surface states of topological insulators. *Nat. Phys.***12**, 1027 (2016).
16. Tao, Q. Liu, B. Miao, R. Yu, Z. Feng, L. Sun, B. You, J. Du, K. Chen, S. Zhang, L. Zhang, Z. Yuan, D. Wu, and H. Ding, Self-consistent determination of spin Hall angle and spin diffusion length in Pt and Pd: The role of the interface spin loss. *Sci. Adv.* **4**, 1670 (2018).
17. Chen, and S. Zhang, Spin Pumping Induced Electric Voltage. *IEEE Magn. Lett.* **6**, 1. (2015).
18. Gannett, M. W. Kellera, H. T. Nembach, T. J. Silva, and A. N. Chiaramonti, Suppression of spin pumping between $Ni_{80}Fe_{20}$and Cu by a graphene interlayer. *J. Appl. Phys.* **117**, 213907 (2015).
19. Zhang, and A. Fert, Conversion between spin and charge currents with topological insulators. *Phys. Rev. B* **94**, 184423 (2016).
20. Dey, N. Prasad, L. F. Register, and S. K. Banerjee, Conversion of spin current into charge current in a topological insulator: Role of the interface. *Phys. Rev. B* **97**, 174406 (2018).
21. Kim, Y.-T. Chen, S. Karube, S. Takahashi, K. Kondou, G. Tatara, and Y. Otani, Evaluation of bulk-interface contributions to Edelstein magnetoresistance at metal/oxide interfaces. *Phys. Rev. B* **96**, 140409(R) (2017).
22. H. Su, P. Y. Chuang, S. W. Chen, H.-Y. Chen, Y. Tung, W.-C. Chen, C.-H. Wang, Y.-W. Yang, J. C. A. Huang, T.-R. Chang, H. Lin, H.-T. Jeng, C.-M. Cheng, K.-D. Tsuei, H. L. Su, and Y. C. Wu, Selective Hydrogen Etching Leads to 2D Bi(111) Bilayers on Bi_2Se_3: Large Rashba Splitting in Topological Insulator Heterostructure. *Chem. Mater.* **29**, 8992 (2017).
23. C. Rojas Sánchez, L. Vila, G. Desfonds, S. Gambarelli, J. P. Attané, J. M. De Teresa, C. Magén, and A. Fert, Spin-to-charge conversion using Rashba coupling at the interface between non-magnetic materials. *Nat. Commun.* 4, 2944 (2013).
24. Zhou, Y. P. Liu, Z. Wang, S. J. Ma, M. W. Jia, R. Q. Wu, L. Zhou, W. Zhang, M. K. Liu, Y. Z. Wu, and J. Qi, Broadband Terahertz Generation via the Interface Inverse Rashba-Edelstein Effect. *Phys. Rev. Lett.* **121**, 086801 (2018).
25. Wang, L. Cheng, D. Zhu, Y. Wu, M. Chen, Y. Wang, D. Zhao, C. B. Boothroyd, Y. M. Lam, J.-X. Zhu, M. Battiato, J. C. W. Song, H. Yang, and E. E. M. Chia, Ultrafast Spin-to-Charge Conversion at the Surface of Topological Insulator Thin Films. *Adv. Mater.* 30, 1802356 (2018).

Figures

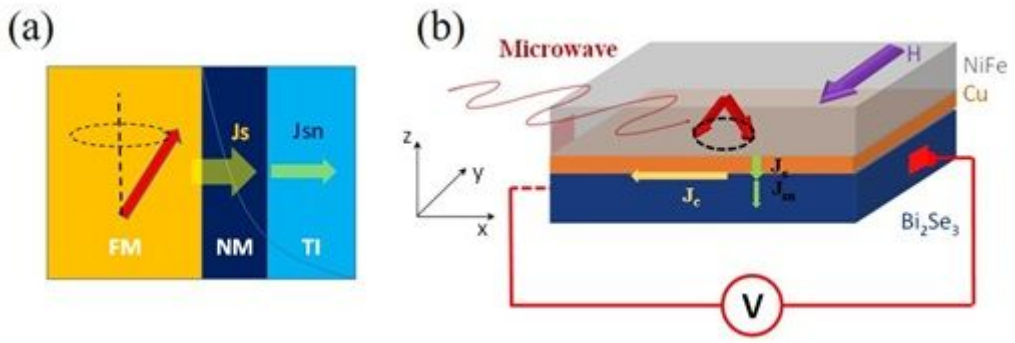

Figure 1

(a) Tri-layer samples for spin pumping study, where nonmagnetic (NM) spacer was introduced in between FM and TI layer; (b) schematic illustrates the spin pumping experiment.

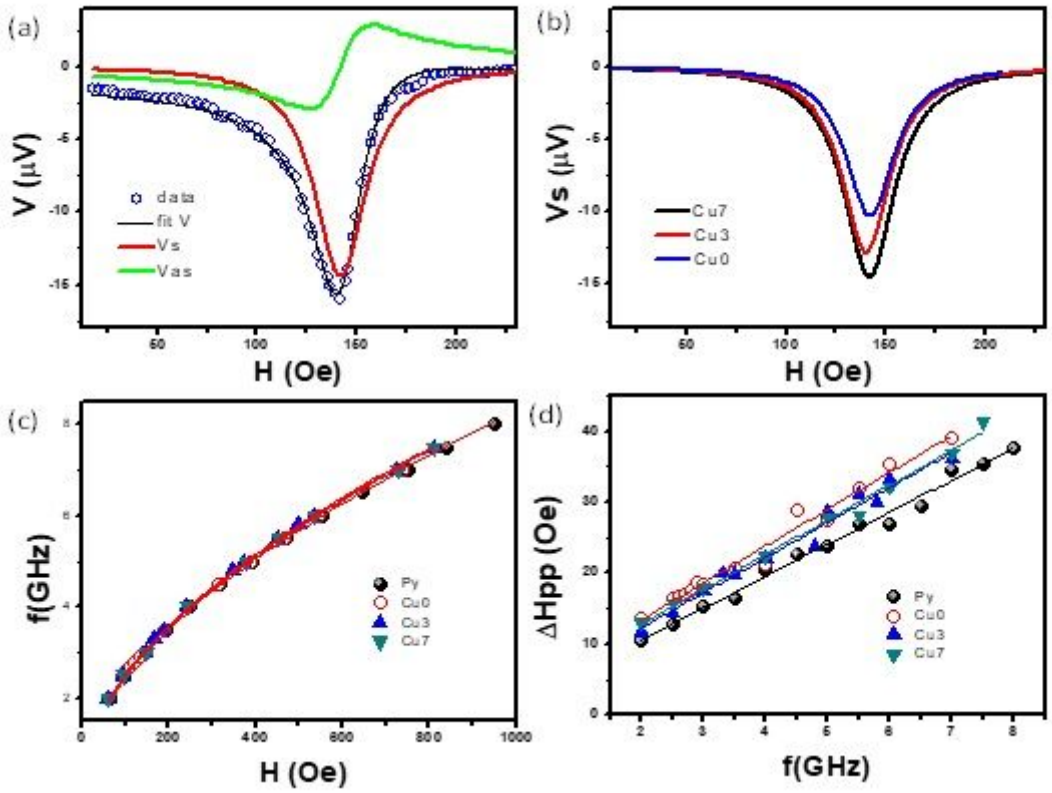

Figure 2

(a) Measured dc voltage at 3GHz for Py/Cu(7nm)/Bi2Se3; (b) extracted Vs for various samples; (c) excitation frequency as a function of resonant field. The solid lines are the fitted curves using Kittel formula; (d) frequency dependence of FMR line width for samples with different Cu thickness. The solid lines show the linear fitting, from which the damping factor(α) of each sample is derived.

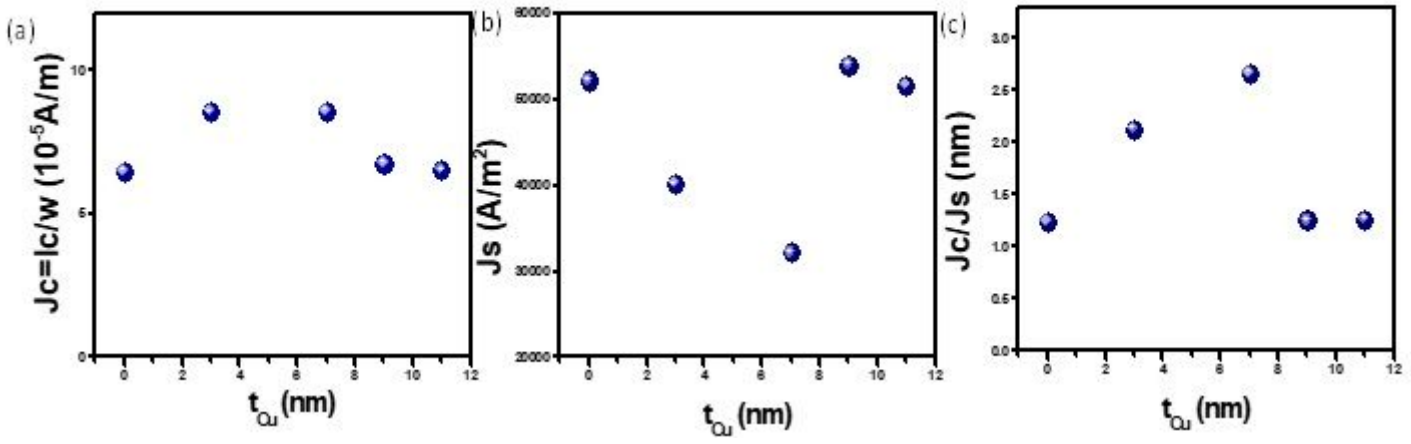

Figure 3

(a) Jc vs tCu; (b) Js vs tCu; (c) Jc/Js vs tCu measured at 3GHz excitation frequency.

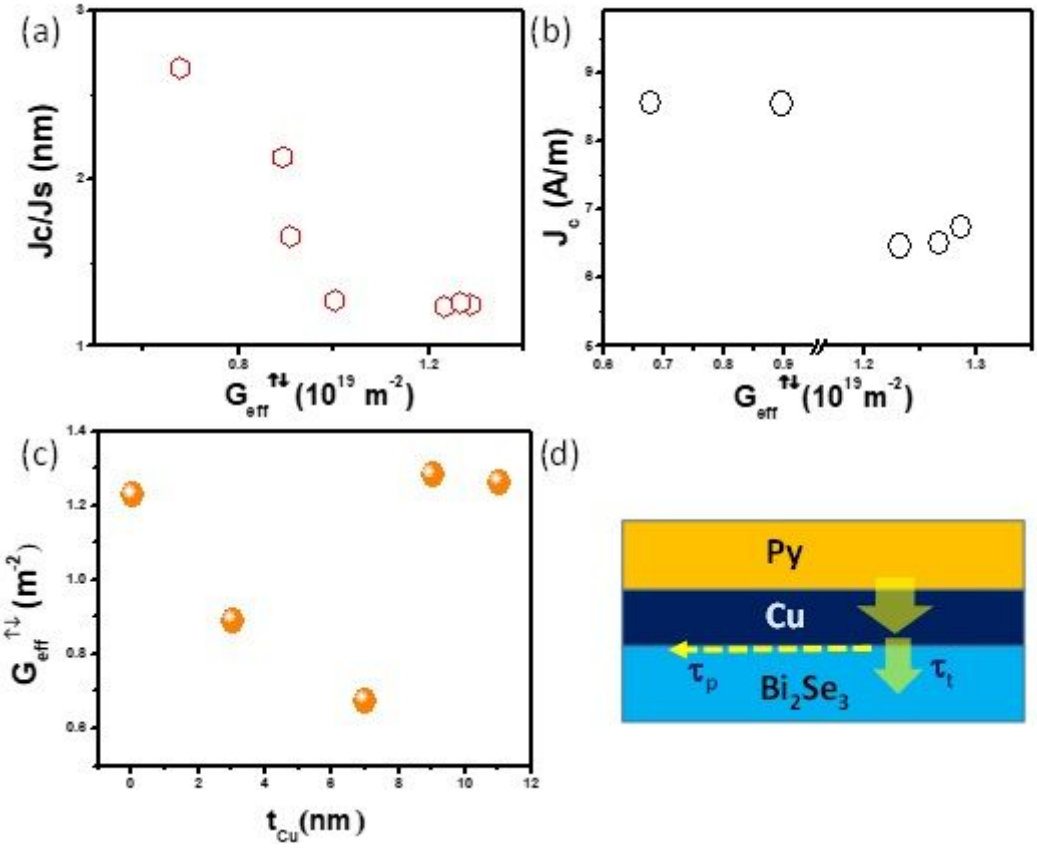

Figure 4

(a) Jc/Js at various Geff⁻; (b) Jc at various Geff⁻; (c) Geff⁻ vs. tCu; (d) schematic illustrates the spin transport in Py/Cu/TI.

Supplementary Files

This is a list of supplementary files associated with this preprint. Click to download.

- Supp.Mater..docx